MICROBIOLOGY

RESEARCH ARTICLE

Margalit *et al.*, *Microbiology* 2022;168:001164

DOI 10.1099/mic.0.001164

MICROBIOLOGY SOCIETY

OPEN ACCESS

Exposure to the *Pseudomonas aeruginosa* secretome alters the proteome and secondary metabolite production of *Aspergillus fumigatus*

Anatte Margalit, David Sheehan, James C. Carolan and Kevin Kavanagh*

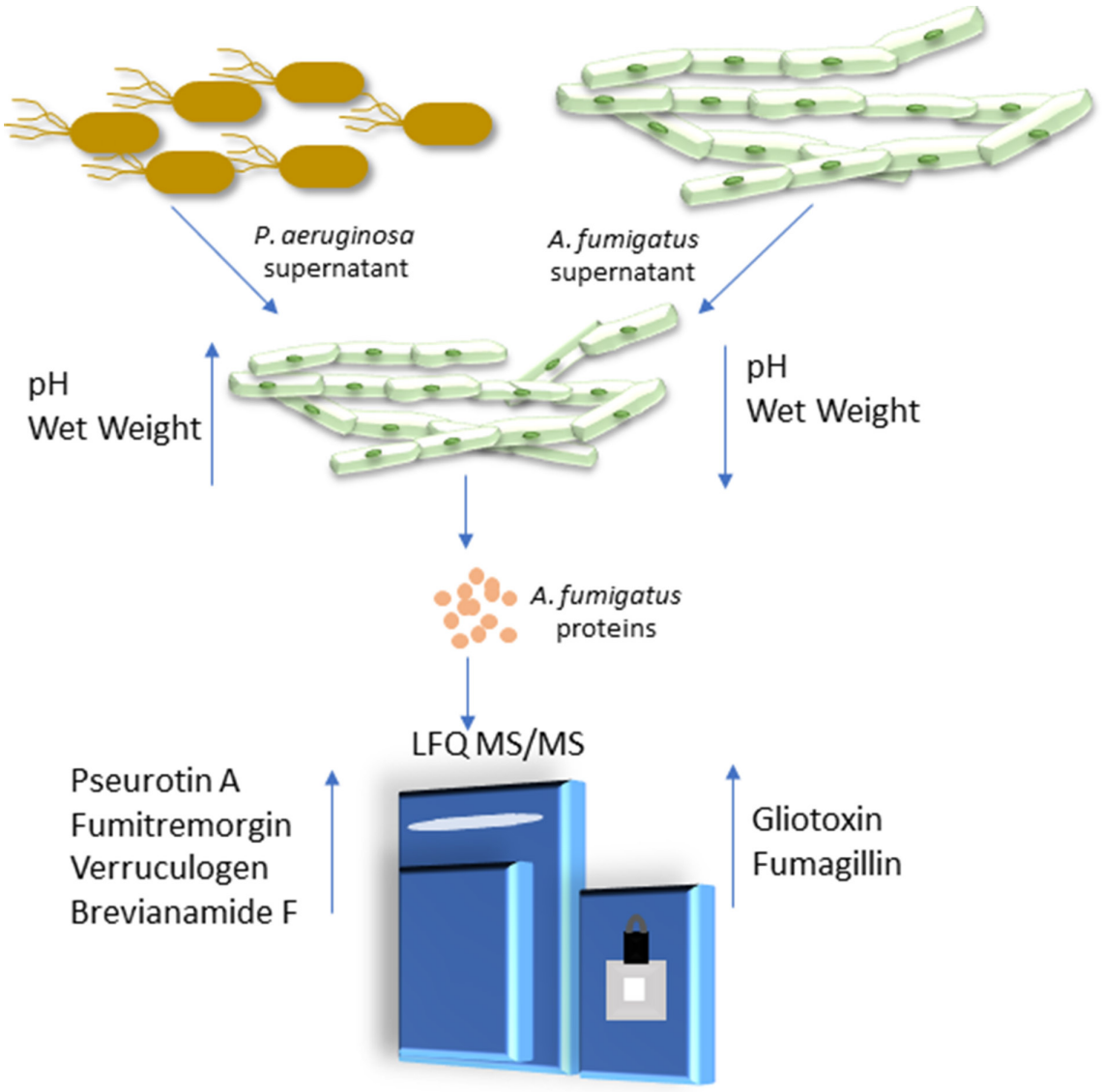

Graphical abstract

The secretome of *P. aeruginosa* or *A. fumigatus* alters the pH of the *A. fumigatus* growth media and affects fungal growth. MS-based proteomic analysis of fungal proteins reveals secretome-dependent changes to the *A. fumigatus* secondary metabolite profile.

Abstract

The fungal pathogen *Aspergillus fumigatus* is frequently cultured from the sputum of cystic fibrosis (CF) patients along with the bacterium *Pseudomonas aeruginosa*. *A. fumigatus* secretes a range of secondary metabolites, and one of these, gliotoxin, has inhibitory effects on the host immune response. The effect of *P. aeruginosa* culture filtrate (CuF) on fungal growth and gliotoxin production was investigated. Exposure of *A. fumigatus* hyphae to *P. aeruginosa* cells induced increased production of gliotoxin and a decrease in fungal growth. In contrast, exposure of *A. fumigatus* hyphae to *P. aeruginosa* CuF led to increased growth and decreased gliotoxin production. Quantitative proteomic analysis was used to characterize the proteomic response of *A. fumigatus* upon exposure to *P. aeruginosa* CuF. Changes in the profile of proteins involved in secondary metabolite biosynthesis (e.g. gliotoxin, fumagillin, pseurotin A), and changes to the abundance of proteins involved in oxidative stress (e.g. formate dehydrogenase) and detoxification (e.g. thioredoxin reductase) were observed, indicating that the bacterial secretome had a profound effect on the fungal proteome. Alterations in the abundance of proteins involved in detoxification and oxidative stress highlight the ability of *A. fumigatus* to differentially regulate protein synthesis in response to environmental stresses imposed by competitors such as *P. aeruginosa*. Such responses may ultimately have serious detrimental effects on the host.

INTRODUCTION

Aspergillus fumigatus is a ubiquitous saprophytic mould that releases airborne conidia, which may enter the human respiratory tract through inhalation. Many of the biological determinants that contribute to the ubiquity of the fungus in nature also play a role in establishing disease in humans and are associated with virulence and pathogenesis [1–6]. Among these attributes are the wide range of biosynthetic gene clusters (>30) responsible for the production of secondary metabolites that confer advantages to *A. fumigatus* in its natural habitat, including protection against UV stress, desiccation and competition with other microorganisms [7–9]. Some of these secondary metabolites may play a role in evading or subverting the host immune response *in vivo,* and consequently many secondary metabolites such as gliotoxin, fumagillin and dihydroxynapthalene (DHN) melanin, and their effects on the host, have been well characterized [7, 9–12].

A. fumigatus is frequently detected in the airways of individuals with cystic fibrosis (CF) from an early age and contributes to the structural damage and disease progression [13–15]. Allergic bronchopulmonary aspergillosis (ABPA) is a hypersensitivity disorder characterized by the induction of a pro-inflammatory immune response triggered by the secretion of fungal toxins and allergens in the airways. It is estimated that 1–2.5% of patients with persistent asthma and 1–15% of CF patients are affected by ABPA [16–18], but this prevalence has probably been underestimated due to under-diagnosis [19].

The most common bacterial pathogen associated with CF, *Pseudomonas aeruginosa*, is a major cause of morbidity and mortality and it is estimated that 60–80% of CF patients experience chronic *P. aeruginosa* infection by the age of 20 years [20–22]. *A. fumigatus* infection is associated with an increased risk of *P. aeruginosa* infection and co-infection is associated with a decline in lung function [14, 21, 23, 24]. The prevalence of co-colonization with *P. aeruginosa* and *A. fumigatus* in the CF airways is estimated to be between 3.1 and 15.8%, although this occurrence may be higher [20, 25, 26].

Co-infection studies have demonstrated that *P. aeruginosa* may inhibit *A. fumigatus* growth *in vivo* and *in vitro* [27–32]. Indirect interaction studies have shown that gliotoxin, produced by *A. fumigatus*, inhibits *P. aeruginosa* growth [33]. However, there is evidence to show that under nutrient-limiting conditions, *A. fumigatus* creates a nutrient-rich environment in which *P. aeruginosa* can rapidly proliferate [34]. A number of studies have been performed to show the effect of volatile organic compounds (VOCs) produced by *P. aeruginosa* on *A. fumigatus* growth [35–37]. The studies revealed contrasting results whereby *P. aeruginosa*-derived sulphur-based VOCs, such as dimethyl sulphide, promote *A. fumigatus* growth [35], while another class of ketone-based VOCs inhibit fungal growth [37]. Differences in growth media, bacterial strains and experimental design probably contribute to the production of different VOCs, explaining the contrasting results of these studies [37]. Nevertheless, the manner in which one pathogen impacts the metabolome of another may have serious implications for the host, as competition between microorganisms can often lead to an altered secretion profile that can have the potential to increase damage to host tissue [38, 39].

Received 13 December 2021; Accepted 16 February 2022; Published 25 March 2022
Author affiliations: [1]Department of Biology, Maynooth University, Co. Kildare, Ireland.
*Correspondence: Kevin Kavanagh, kevin.kavanagh@mu.ie
Keywords: *Aspergillus*; gliotoxin; infection; *Pseudomonas*; proteomics.
Abbreviations: ABPA, allergic bronchopulmonary aspergillosis; CF, cystic fibrosis; CuF, culture filtrate; GS, glyoxylate shunt; LFQ, label-free quantitative; PCA, principal components analysis; RP-HPLC, reversed-phase HPLC; SSDA, statistically significant differentially abundant; TC, tricarboxylic cycle; VOC, volatile organic compound.
Four supplementary tables and one supplementary figure are available with the online version of this article.

Although numerous interaction studies have been performed between these pathogens, the influence of the *P. aeruginosa* secretome on the *A. fumigatus* proteome and secondary metabolite production has not been fully characterized to date. In this study, label-free quantitative MS was used to investigate how *A. fumigatus* responds to *P. aeruginosa* culture filtrate (CuF) produced under nutrient-limiting, nitrate-rich conditions. Understanding the interactions that occur between these pathogens is vital to the development of therapeutic targets that will minimize the contribution of these pathogens, individually and collectively, to disease progression.

METHODS

Pseudomonas aeruginosa cultures

P. aeruginosa (PAO1) was cultivated on nutrient agar (Oxoid) or in nutrient broth (Oxoid) at 37 °C. Bacterial cultures were grown to stationary phase (48 h) at 37 °C in an orbital incubator (200 r.p.m.). The concentration of the bacterial suspension was measured by obtaining the optical density at 600 nm (OD_{600}), and an OD of 1 equated to 3×10^8 c.f.u. ml^{-1}.

Aspergillus fumigatus cultures

A. fumigatus (ATCC 26933) was grown on Sabouraud dextrose agar (Oxoid) at 37 °C. Conidia were harvested using 0.01% (v/v) Tween-80 and washed twice with PBS. Conidial density was ascertained by haemocytometry and conidia were added to Czapek-Dox liquid media to give a density of 5×10^5 ml^{-1}. The cultures were incubated for 48 h at 37 °C in an orbital incubator at 200 r.p.m.

Preparation of *P. aeruginosa* culture filtrates

Czapek-Dox liquid media (pH 6.8) (Duchefa, Biochemi) was inoculated with *P. aeruginosa* and incubated for 48 h at 37 °C in an orbital incubator, at 200 r.p.m. The bacteria were harvested by centrifugation (15 min, 2000 ***g***). *P. aeruginosa* CuF was sterilized using 0.2 µm filtropur S filters (Sarstedt) and the pH was measured (pH 7.2).

Preparation of *A. fumigatus* culture filtrate

A. fumigatus conidia (5×10^5 ml^{-1}) were added to Czapek-Dox liquid media (pH 6.8). The cultures were incubated for 48 h at 37 °C in an orbital incubator at 200 r.p.m. The hyphal mass was harvested and the wet weight was recorded. The *A. fumigatus* CuF was sterilized using 0.2 µm filtropur S filters (Sarstedt) and the pH was measured (4.5).

Exposure of *A. fumigatus* to culture filtrates

A. fumigatus conidia (5×10^5 conidia ml^{-1} in 25 ml Czapek-Dox liquid media) were cultured for 4 h in Czapek-Dox liquid media until germination occurred (verified microscopically). *A. fumigatus* CuF or *P. aeruginosa* CuF (50 ml) were added to the fungal cultures (n=4) to give a final volume of 75 ml (66% CuF to 33% starting culture). The fungal cultures were incubated for 24 h at 37 °C in an orbital incubator (200 r.p.m.).

Extraction of gliotoxin from *P. aeruginosa*-exposed and CuF-exposed *A. fumigatus* cultures

Filtrates obtained from *A. fumigatus* cultures that had been exposed to various concentrations of *P. aeruginosa*, *A. fumigatus* or *P. aeruginosa* CuF (n=4) were mixed with an equal volume (20 ml) of chloroform (Fisher Chemical) for 2 h at room temperature. The chloroform fraction was collected and dried by rotary evaporation in a Büchi rotor evaporator (Brinkmann Instruments). Dried extracts were dissolved in 500 µl methanol (Fisher Chemical) and stored at −20 °C.

Quantification of gliotoxin by RP-HPLC

Gliotoxin was detected by reversed phase-HPLC (RP-HPLC; Shimadzu). The mobile phase was 34.9% (v/v) acetonitrile (Fisher Scientific), 0.1% (v/v) trifluoroacetic acid (TFA) (Sigma Aldrich) and 65% (v/v) HPLC-grade water (ddH_2O). Gliotoxin extract (20 µl) (Sigma Aldrich) was injected onto a Lunar Omega, 5 µm polar C18, LC column (Phenomenex). A standard curve of peak area versus gliotoxin concentration was constructed using gliotoxin standards (0.1, 0.25, 0.5 and 1.0 µg per 10 µl) dissolved in methanol (Sigma Aldrich).

Protein extraction from *A. fumigatus* hyphae

A. fumigatus hyphae from each CuF-exposed treatment (n=4) were crushed to a fine dust with liquid nitrogen in a mortar using a pestle. Lysis buffer (4 ml g^{-1} hyphae) [8 M urea, 2 M thiourea, and 0.1 M Tris-HCl (pH 8.0) dissolved in HPLC-grade dH_2O], supplemented with protease inhibitors [aprotinin, leupeptin, pepstatin A, and Tosyllysine Chloromethyl Ketone hydrochloride (TLCK) (10 µg ml^{-1}) and PMSF (1 mM ml^{-1})] was added to the crushed hyphae. Cell lysates were sonicated (Bendelin Senopuls), three times for 10 s at 50% power. The cell lysate was subjected to centrifugation (Eppendorf Centrifuge 5418) for 8 min at 14500 ***g*** to pellet cellular debris. The supernatant was removed and quantified using the Bradford method. Samples (100 µg) were subjected to overnight acetone precipitation.

Label-free MS (LF/MS)

A. fumigatus proteins were pelleted by centrifugation for 10 min at 14500 ***g***. The acetone was removed and the protein pellet was re-suspended in 25 µl sample resuspension buffer [8 M urea, 2 M thiourea, 0.1 M Tris-HCl (pH 8.0) dissolved in HPLC-grade dH_2O]. An aliquot (2 µl) was removed from each sample and quantified using the Qubit quantification system (Invitrogen), following the manufacturer's instructions. Ammonium bicarbonate (125 µl, 50 mM) was added to the remaining 20 µl of each sample. The protein sample was reduced by adding 1 µl 0.5 M DTT and incubated at 56 °C for 20 min, followed by alkylation with 0.55 M iodoacetamide at room temperature, in the dark for 15 min. Protease Max Surfactant Trypsin Enhancer (Promega) (1 µl, 1 % w/v) and Sequence Grade Trypsin (Promega) (0.5 µg μl^{-1}) was added to the proteins and incubated at 37 °C for 18 h. Digestion was terminated by adding TFA (1 µl, 100%) to each tryptic digest sample, and incubated at room temperature for 5 min. Samples were centrifuged for 10 min at 14500 ***g*** and purified for MS using C18 Spin Columns (Pierce), following the manufacturer's instructions. The eluted peptides were dried using a SpeedyVac concentrator (Thermo Scientific Savant DNA120) and resuspended in 2% (v/v) acetonitrile and 0.05% (v/v) TFA to give a final peptide concentration of 1 µg μl^{-1}. The samples were sonicated for 5 min to aid peptide resuspension, followed by centrifugation for 5 min at 14500 ***g***. The supernatant was removed and used for MS. Three independent biological replicates for each group were analysed in this study.

Protein extraction from *P. aeruginosa* culture filtrates

Aliquots of *P. aeruginosa* culture filtrates were subjected to overnight acetone precipitation. Precipitated proteins were pooled together and resuspened with lysis buffer (total 250 µl) containing protease inhibitors as described above. An aliquot (2 µl) was removed from the lysate and quantified using the Qubit quantification system (Invitrogen). Samples (50 µg) were subjected to a further overnight acetone precipitation step and prepared for analysis by LC-MS as described above.

MS: LC/MS Xcalibur Instrument parameters for *A. fumigatus* proteomic data acquisition

Each digested *A. fumigatus* protein sample (750 ng) and *P. aeruginosa* CuF sample (500 ng) was loaded onto a QExactive (ThermoFisher Scientific) high-resolution accurate MS device connected to a Dionex Ultimate 3000 (RSLCnano) chromatography system. Peptides were separated by an increasing acetonitrile gradient on a 50 cm EASY-Spray PepMap C18 column of 75 µm diameter (2 µm particle size), using a 133 min (*A. fumigatus* proteins) and 65 min (*P. aeruginosa* CuF proteins) reversed-phase gradient at a flow rate of 300 nl min^{-1}. All data were acquired with the MS device operating in an automatic-dependent switching mode. A full MS scan at 70000 resolution and a range of 400–1600 m/z was followed by an MS/MS scan at 17500 resolution, with a range of 200–2000 m/z to select the 15 most intense ions prior to MS/MS.

Quantitative analysis (protein quantification and LFQ normalization of the MS/MS data) of the *A. fumigatus* proteome arising from exposure to the different CuFs was performed using MaxQuant version 1.5.3.3 (http://www.maxquant.org) following the general procedures and settings outlined previously [40]. The Andromeda search algorithm incorporated in the MaxQuant software was used to correlate MS/MS data against the Uniprot-SWISS-PROT database for *A. fumigatus* Af293 (downloaded 11 September 2018; 9648 entries). The following search parameters were used: first search peptide tolerance of 20 ppm, second search peptide tolerance of 4.5 ppm with cysteine carbamidomethylation as a fixed modification and N-acetylation of protein and oxidation of methionine as variable modifications and a maximum of two missed cleavage sites allowed. The false discovery rate (FDR) was set to 1% for both peptides and proteins, and the FDR was estimated following searches against a target-decoy database. Peptides with minimum length of 7 aa were considered for identification and proteins were only considered identified when observed in three replicates of one sample group.

Data analysis of the *A. fumigatus* proteome

Perseus v.1.5.5.3 (www.maxquant.org/) was used for data analysis, processing and visualization. Normalized LFQ intensity values were used as the quantitative measurement of protein abundance for subsequent analysis. The data matrix was first filtered to remove contaminants and peptides identified by site. LFQ intensity values were log_2-transformed and each sample was assigned to its corresponding group, i.e. *A. fumigatus* exposed to *A. fumigatus* CuF versus *P. aeruginosa* CuF. Proteins not found in three out of three replicates in at least one group were omitted from the analysis. A data-imputation step was conducted to replace missing values with values that simulate signals of low-abundance proteins chosen randomly from a distribution specified by a downshift of 1.8 times the mean standard deviation (SD) of all measured values and a width of 0.3 times this SD. Normalized intensity values were used for a principal component analysis (PCA). Exclusively expressed proteins (those that were uniquely expressed or completely absent in one group) were identified from the pre-imputation dataset and included in subsequent analyses. Gene ontology (GO) mapping was also performed in Perseus using the UniProt gene ID for all identified proteins to query the Perseus annotation file (downloaded September 2018) and extract terms for biological process, molecular function and Kyoto Encyclopaedia of Genes and Genomes (KEGG) name.

To visualize differences between two samples, pairwise Student's t-tests were performed for all using a cut-off of $P<0.05$ on the post-imputated dataset. Volcano plots were generated in Perseus by plotting negative log P-values on the y-axis and log2 fold-change values on the x-axis for each pairwise comparison. The 'categories' function in Perseus was utilized to highlight and

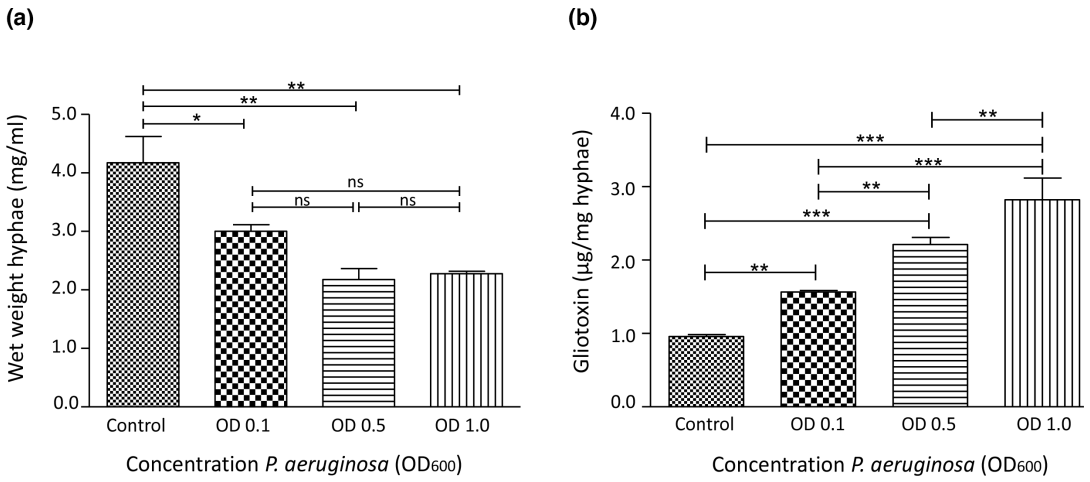

Fig. 1. The effect of *P. aeruginosa* cells on *A. fumigatus* hyphal growth and gliotoxin production. (a) *A. fumigatus* hyphae (wet weight mg ml^{-1}) after co-incubation for 24 h with nutrient broth (control, 1 ml) or *P. aeruginosa* cell suspension (OD_{600} 0.1, 0.5, 1.0; 1 ml). (b) Gliotoxin (µg mg^{-1} hyphae) produced by *A. fumigatus* in Czapek-Dox liquid media supplemented with nutrient broth (control, 1 ml) or *P. aeruginosa* cell suspension (OD_{600} 0.1, 0.5, 1.0; 1 ml) measured by RP-HPLC. ***P<0.001, **P<0.01, *P<0.05, ns: non-significant.

visualize the distribution of various pathways and processes on selected volcano plots. Statistically significant (ANOVA, P<0.05) and differentially abundant proteins [statistically significant differentially abundant (SSDA)], i.e. with fold change of plus or minus 1.5, were chosen for further analysis.

The MS proteomics data and MaxQuant search output files have been deposited with the ProteomeXchange Consortium [41] via the PRIDE partner repository with the dataset identifier PXD030171.

Data analysis of the *P. aeruginosa* CuF secretome

Qualitative analysis of the proteome arising from the *P. aeruginosa* CuF was investigated using Proteome Discoverer 1.4 and Sequest HT (SEQUEST HT algorithm; Thermo Scientific). Identified proteins were searched against the UniProtKB database (*Pseudomonas aeruginosa*; 5564 entries). Search parameters applied for protein identification were as follows: (i) enzyme name – trypsin, (ii) an allowance of up to two missed cleavages, (iii) peptide mass tolerance set to 10 ppm, (iv) MS/MS mass tolerance set to 0.02 Da, (v) carbamidomethylation set as a fixed modification and (vi) methionine oxidation set as a variable modification . Peptide probability was set to high confidence (with an FDR≤0.01% as determined by Percolator validation in Proteome Discoverer). Peptides with a minimum score of two and fewer than two unique peptides were excluded from further analysis [42]. The MS proteomics data and Proteome Discoverer search output files have been deposited with the ProteomeXchange Consortium via the PRIDE partner repository with the dataset identifier PXD031565.

Statistical analysis

The effect of *P. aeruginosa* on *A. fumigatus* growth was analysed using GraphPad Prism 5. One-way ANOVA with Tukey's multiple comparisons test was performed to compare the growth of hyphae exposed to different bacterial densities and CuFs, and the effect on gliotoxin production. P values <0.05 were considered significant.

RESULTS

Analysis of the effect of *P. aeruginosa* on *A. fumigatus* growth and gliotoxin production

The addition of *P. aeruginosa* cells to a culture of ungerminated conidia inhibited the growth of *A. fumigatus,* and as such, data could not be obtained to examine the *P. aeruginosa*–*A. fumigatus* interaction. To measure the effect of *P. aeruginosa* cells on *A. fumigatus* growth, different concentrations of *P. aeruginosa* (1 ml OD 1.0, which equates to approximately 3×10^8 cells ml^{-1}, OD 0.5 and OD 0.1) were added to established (48 h) *A. fumigatus* cultures grown in Czapek-Dox medium (100 ml). The co-cultures were incubated for 24 h after which the effect on fungal growth was measured by obtaining the wet weight of the hyphae (Fig. 1a). Gliotoxin was extracted from each group of bacteria-exposed *A. fumigatus* cultures and quantified by RP-HPLC (Fig. 1b). The decrease in wet weight and an increase in gliotoxin production correlated with the increase in *P. aeruginosa* cell density. The wet weights of fungal cultures exposed to the highest concentration of *P. aeruginosa* (OD 1) (9.1±0.3 mg ml^{-1}) were 46% lower

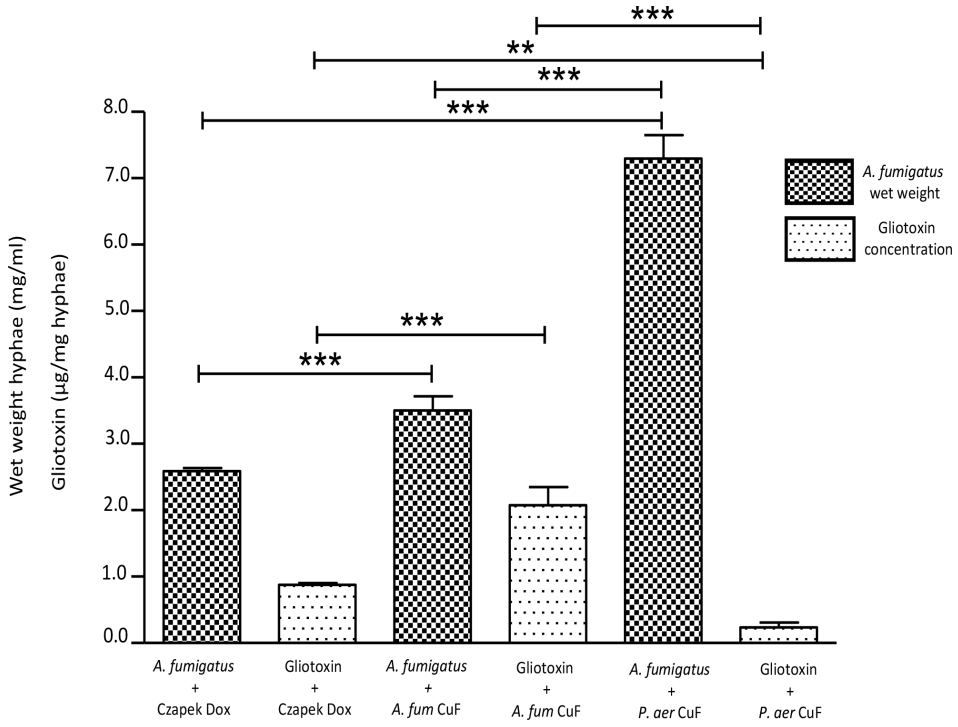

Fig. 2. The effect of *P. aeruginosa* CuF on early stages of *A. fumigatus* growth and gliotoxin production. *A. fumigatus* germinating conidia grown in Czapek-Dox media for 4 h prior to exposure to non-supplemented media (sterile Czapek-Dox), *A. fumigatus* CuF or *P. aeruginosa* CuF for 24 h. Fungal growth was measured as wet weight (mg ml^{-1}). Gliotoxin (µg ml^{-1}) was extracted from fungal cultures after 24 h and measured by RP-HPLC ***P<0.001, **P<0.01.

than the controls (16.7±3.1 mg ml^{-1}). The level of gliotoxin produced by *A. fumigatus* exposed to these bacterial densities was 2.82±0.3 µg mg^{-1}. In contrast, the level of gliotoxin produced by the control cultures was three-fold lower (0.96±0.03 µg mg^{-1}).

To investigate the effect of the *P. aeruginosa* secretome on growth of *A. fumigatus*, conidia were allowed to germinate in Czapek-Dox liquid media for 4 h, and then supplemented with the culture filtrate produced by *P. aeruginosa* grown in Czapek-Dox for 48 h (*P. aeruginosa* CuF). *A. fumigatus* growth was greater after exposure to *P. aeruginosa* CuF (6.93±0.25 mg ml^{-1}) compared to growth in *A. fumigatus* CuF (3.5±0.21 mg ml^{-1}) or non-supplemented media (2.58±0.05 mg ml^{-1}) (Fig. 2). The highest concentrations of gliotoxin were detected in the supernatants of the fungal cultures exposed to *A. fumigatus* CuF (2.1±0.27 µg mg^{-1} hyphae) followed by those exposed to non-supplemented media (0.88±0.027 µg mg^{-1} hyphae) and *P. aeruginosa* CuF (0.24±0.07 µg mg^{-1} hyphae), respectively (Fig. 2).

To investigate whether the differences in fungal growth were caused by differences in pH of the *A. fumigatus* and *P. aeruginosa* secretome, the pH of the CuFs was determined. The pH of sterile Czapek-Dox medium was adjusted to that of the *A. fumigatus* secretome (pH 4.5) and *P. aeruginosa* secretome (pH 7.2). Conidia were cultured for 4 h as described previously prior to being exposed to the pH-adjusted Czapek-Dox medium. The pH and the wet weight of the fungus were measured after 24 h (Fig. S1, available in the online version of this article), and indicate that pH did not affect the growth of *A. fumigatus*.

Analysis of the *P. aeruginosa* secretome by MS

The protein content of the culture filtrates produced by *P. aeruginosa* was analysed by high-resolution MS. In total, 402 proteins were detected, of which 134 remained after filtering. The proteomic analysis revealed a range of enzymes involved in amino acid metabolism (glutamine synthetase, malate synthase G, arginine deiminase) and ATP synthesis (ATP synthase subunit alpha and beta, ubiquinol-cytochrome *c* reductase) protein chaperones (chaperone protein DnaK, chaperone SurA, 10 kDa chaperonin, chaperone protein ClpB, trigger factor) and with the uptake of nutrients including iron (ferric iron-binding periplasmic protein HitA) and amino acids [amino acid (lysine/arginine/ornithine/histidine/octopine) ABC transporter periplasmic binding protein, leucine-, isoleucine-, valine-, threonine- and alanine-binding protein]. Proteins involved with the glyoxylate shunt were also detected, including malate synthase G and isocitrate lyase. Several proteins associated with detoxification (catalase, thioredoxin, glutathione peroxidase, xenobiotic reductase and thiol:disulphide interchange protein DsbA) and redox regulation (isocitrate dehydrogenase, citrate synthase and oxoglutarate dehydrogenase) were identified in the dataset (Dataset S1).

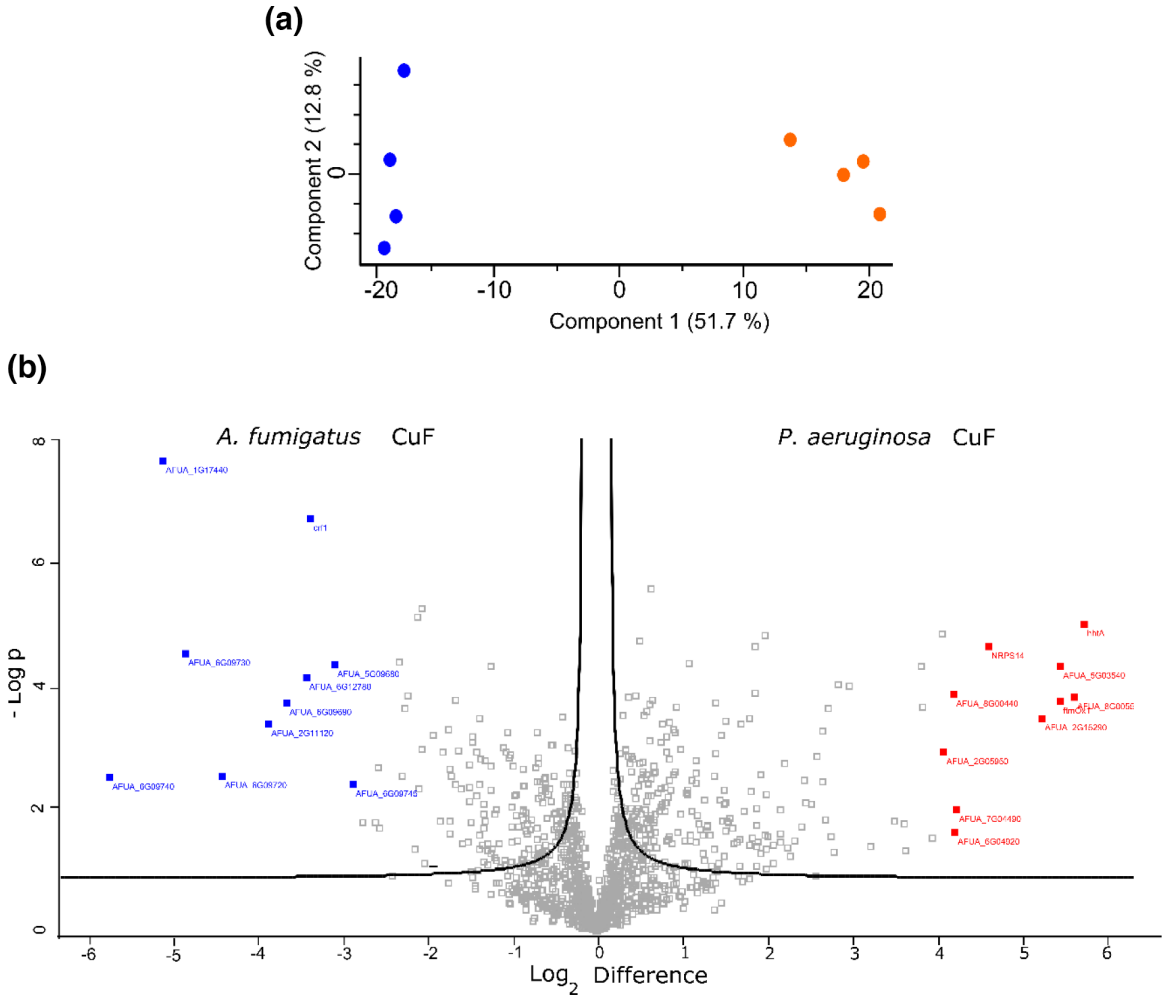

Fig. 3. (a) PCA of *A. fumigatus* protein groups. PCA of *A. fumigatus* exposed to *A. fumigatus* CuF (blue) and *P. aeruginosa* CuF (orange). A clear distinction can be observed between each of the groups exposed to *P. aeruginosa* CuF and *A. fumigatus* CuF. (b) Differential abundance of proteins in the *A. fumigatus* proteome. Volcano plots derived from pairwise comparisons between *A. fumigatus* cultured in *P. aeruginosa* CuF and *A. fumigatus* CuF. The distribution of quantified proteins according to *P* value ($-\log_{10}$ *P*-value) and fold change ($\log_2$ mean LFQ intensity difference) is shown. Proteins above the line are considered statistically significant ($P<0.05$). The top 10 statistically significant proteins that increased in abundance are highlighted in red. The top 10 statistically significant proteins that decreased in abundance are highlighted in blue. The gene names are included beside each protein.

The proteomic response of *A. fumigatus* to *P. aeruginosa* CuF

Changes to the proteome of *A. fumigatus* in response to *P. aeruginosa* CuF were investigated by LFQ proteomics, which was performed on *A. fumigatus* exposed to *P. aeruginosa* CuF, and *A. fumigatus* CuF (control) ($n=4$). In total, 2414 proteins were identified, of which 1373 remained after filtering and processing (Dataset S2). Of the 1373 proteins identified post-imputation, a comparison between the two groups yielded 272 proteins which were determined to be statistically significant ($P<0.05$) differentially abundant (SSDA) with a fold change of ±1.5 (Dataset S3). A PCA was performed on all filtered proteins and identified distinct proteomic differences between the groups (Fig. 3a). Components 1 and 2 accounted for 64.5% of the total variance within the data, and all replicates resolved into their corresponding samples. The groups exposed to *A. fumigatus* CuF (control) displayed a clear difference from those that were challenged with *P. aeruginosa* CuF.

Volcano plots were produced by pairwise Student's *t*-tests ($P<0.05$) to determine the differences in protein abundance between two samples and to depict the changes in pathways and processes in which those proteins are involved (Fig. 3b). The top 10 proteins that most increased and decreased in relative abundance are highlighted in the volcano plot and listed in Table 1. SSDA protein names arising from the pairwise *t*-tests were inputted into Uniprot (uniprot.org) and used to identify the GO terms and metabolic pathways to which proteins belonged.

Table 1. Relative fold differences of the top 20 SSDA (*t*-test, *P*<0.05) proteins detected in the proteomic dataset arising from *A. fumigatus* groups exposed to *A. fumigatus* CuF and *P. aeruginosa* CuF

Gene	Protein name	Fold change
hhtA	Histone H3	+53.81
AFUA_1G17440 (psoC) ftmOx1	Methyltransferase psoC	+49.55
AFUA_5G03540	Verruculogen synthase	+44.10
AFUA_2G15290	Thioredoxin reductase, putative	+43.91
NRPS14	DUF636 domain protein	+37.79
AFUA_7G04490	Non-ribosomal peptide synthetase 14	+24.69
AFUA_6G04920	Ribosomal protein S28e	+18.90
AFUA_8G00440 (psoF)	Formate dehydrogenase	+18.64
	Dual-functional monooxygenase/methyltransferase psoF	+18.35
(AFUA_6G09740) gliT	Thioredoxin reductase gliT	−53.23
AFUA_1G17440	ABC multidrug transporter A-1	−34.45
AFUA_6G09730 (gliF)	Cytochrome P450 monooxygenase gliF	−28.47
AFUA_6G09720 (gliN)	*N*-Methyltransferase gliN	−21.13
AFUA_2G11120	Uncharacterized protein	−14.49
AFUA_6G09690 (gliG)	Glutathione *S*-transferase gliG	−12.55
AFUA_6G12780	Uncharacterized protein	−10.58
crf2	Probable glycosidase crf2	−10.34
AFUA_5G09680	Succinate dehydrogenase cytochrome b560 subunit	−8.45
AFUA_6G09745	Uncharacterized protein	−7.26
AFUA_5G01880	Uncharacterized protein	−6.75

The data arising from Student's *t*-tests (*P*<0.05) revealed distinct differences in the proteomic response of *A. fumigatus* when exposed to the *P. aeruginosa* culture filtrate compared with that of its own (Dataset S3). These differences were most evident in the changes to the proteomic profile of secondary metabolites. The relative abundance of proteins involved in pseurotin A biosynthesis [methyltransferase psoC (+49.55-fold), PKS-NRPS hybrid synthetase psoA (+24.69-fold), methyltransferase psoF (+18.35-fold), glutathione *S*-transferase psoE (+5.37-fold)], verruculogen [verruculogen synthase (+44.10-fold)] and fumitremorgin biosynthesis [6-hydroxytryprostatin B *O*-methyltransferase (+11.45-fold)] and brevianamide F [tryprostatin B synthase (+3.69-fold)] were increased significantly (Table 2). In contrast, the relative abundances of several proteins involved in gliotoxin biosynthesis were significantly decreased in *A. fumigatus* cultures exposed to *P. aeruginosa* CuF compared to *A. fumigatus* CuF. These included the protein products of gliF (−28.47-fold), gliG (−12.55-fold), gliN (−21.13-fold) and gliT (−52.23-fold) (Table 2). Other proteins involved in detoxification pathways included GST N-terminal domain-containing protein (−1.81-fold), Peptide-methionine (*S*)-S-oxide reductase (−4.86-fold) and DNA damage response protein (Dap1) (−3.32-fold).

Table 2. Changes in the abundance of proteins associated with secondary metabolite biosynthesis: relative fold differences of SSDA (*t*-test, *P*<0.05) proteins associated with secondary metabolite biosynthesis between *A. fumigatus* groups exposed to *A. fumigatus* CuF and *P. aeruginosa* CuF

Gene	Protein name	Fold change
AFUA_1G17440 (psoC)	Methyltransferase psoC	+49.55
ftmOx1	Verruculogen synthase	+44.10
NRPS14	PKS-NRPS hybrid synthetase psoA	+24.69
AFUA_8G00440 (psoF)	Methyltransferase psoF	+18.35
ftmMT	6-Hydroxytryprostatin B *O*-methyltransferase	+11.45
af390-400	*O*-Methyltransferase af390-400	+7.18
(AFUA_8G00580) psoE	Glutathione *S*-transferase psoE	+5.37
af380	Polyketide transferase af380	+4.24
ftmPT1	Tryprostatin B synthase	+3.69
AFUA_5G04080	Terpene cyclase	+1.54
(AFUA_6G09740) gliT	Thioredoxin reductase gliT	−53.23
(AFUA_6G09730) gliF	Cytochrome P450 monooxygenase gliF	−28.47
(AFUA_6G09720) gliN	*N*-Methyltransferase gliN	−21.13
(AFUA_6G09690) gliG	Glutathione *S*-transferase gliG	−12.55

Table 3. Changes to the *A. fumigatus* stress response pathway: relative fold differences of SSDA (*t*-test, $P<0.05$) proteins associated with a general stress response and mitochondria-related oxidative stress between *A. fumigatus* groups exposed to *P. aeruginosa* CuF and *A. fumigatus* CuF

Gene	Protein	Fold change
AFUA_5G03540	Thioredoxin reductase	+43.91
AFUA_6G04920	Formate dehydrogenase	+18.64
AFUA_3G14540	Heat shock protein Hsp30/Hsp42	+6.67
AFUA_5G09330	CipC-like antibiotic response protein, putative	+6.08
AFUA_8G06080	Nitric oxide dioxygenase	+3.75
katG	Catalase-peroxidase	+3.64
AFUA_3G12560	Allantoicase Alc	+3.27
AFUA_1G08880	Iron/copper transporter Atx1	+3.22
AFUA_4G03120	Mitochondrial cytochrome b2, putative	+2.93
AFUA_4G11250	Carbonic anhydrase	+2.27
AFUA_7G02070	AIF-like mitochondrial oxidoreductase	+2.25
AFUA_2G05060	Alternative oxidase	+1.95
Pmp20	Putative peroxiredoxin pmp20	+1.89
AFUA_4G03900	Peroxisomal multifunctional beta-oxidation protein	+1.83
Atg8	Autophagy-related protein 8	+1.80
AFUA_1G11180	Heat shock protein/chaperonin HSP78, putative	+1.56
svf1	Survival factor 1	+1.54
AFUA_5G09680	Succinate dehydrogenase cytochrome b560 subunit	−8.45
AFUA_4G11390	Ubiquinol-cytochrome *c* reductase complex 17 kd protein	−5.85
AFUA_2G13110	Cytochrome *c*	−1.94
AFUA_4G06790	Cytochrome *b*-*c*1 complex subunit 7	−1.83
AFUA_3G06190	Cytochrome *c* oxidase subunit VIa, putative	−1.54
AFUA_2G11750	Mitochondrial DnaJ chaperone (Mdj1), putative	−1.51

The proteomic data revealed several differentially abundant proteins typically associated with the cellular response to stress in *A. fumigatus* cultures exposed to *P. aeruginosa* CuF. There were clear differences in the type of stress-response proteins, with one group showing an increase in the abundance of proteins involved in a general stress response [e.g. thioredoxin (+43.91-fold), catalase (+3.64-fold), formate dehydrogenase (+18.64-fold)] in *A. fumigatus* exposed to *P. aeruginosa* CuF. The other group of stress-related proteins were involved in mitochondrial-induced stress and included decreased levels of cytochrome proteins in the fungal cultures exposed to *P. aeruginosa* CuF compared to those exposed to *A. fumigatus* CuF (Table 3).

The proteomic dataset revealed significant changes in the abundance of proteins involved with transcriptional and translational regulation. These included ribosomal proteins belonging to the large and small ribosome (ribosomal protein S28e; +18.9fold), 60S ribosomal protein L36; +15.59-fold), proteins involved in splicing (U6 snRNA-associated Sm-like protein LSm6; +2.84-fold, pre-mRNA-splicing factor rse1; +2.07-fold), histone proteins (histone H3; +53.81-fold, histone H2B; +2.29-fold), and regulatory proteins such as translation initiation (eukaryotic translation initiation factor 4C; +4.63-fold) and elongation factors (eukaryotic translation elongation factor 1 subunit Eef1-beta; +1.70-fold). While the greatest changes were detected in the groups that had increased in relative abundance, there were a large proportion of proteins belonging to this group that had also decreased in relative abundance in *A. fumigatus* exposed to *P. aeruginosa* CuF (40S ribosomal protein S2; −4.31-fold, 60S acidic ribosomal protein P2; −4.15-fold, 50S ribosomal protein L13; −3.16-fold, eukaryotic translation initiation factor 3 subunit K; −3.31-fold) (Table S1, Dataset S3).

DISCUSSION

The inhibitory effects of *P. aeruginosa* cells and *P. aeruginosa* secondary metabolites on *A. fumigatus* biofilm formation and fungal growth and development are well established [27, 28, 37, 43, 44]. However, the proteomic response of *A. fumigatus* to the *P. aeruginosa* secreteome remains largely uncharacterized. The results presented in this study demonstrate distinct differences in fungal growth and gliotoxin production where *A. fumigatus* is exposed to *P. aeruginosa* cells, compared to its exposure to *P. aeruginosa* CuF. We chose to use a nutrient-poor, nitrate-rich liquid medium, Czapek-Dox, in which to culture *A. fumigatus* and to produce the *P. aeruginosa* culture filtrates. Czapek-Dox is used to promote the production of redox-active secondary metabolites such as gliotoxin [34, 45, 46] and provides a nitrate-rich environment, which is a feature of CF airways [34, 45–47].

Exposure of *A. fumigatus* to *P. aeruginosa* cells resulted in reduced fungal growth and an increase in gliotoxin production. The growth-inhibiting effect of *P. aeruginosa* on *A. fumigatus* has been reported previously [28, 29, 39, 48, 49]. Rhamnolipids are a family of glycolipids produced by *P. aeruginosa* and other *Pseudomonas* species [50]. Dirhamnolipids produced by *P. aeruginosa* inhibit β 1, 3-glucan synthase, thereby interfering with fungal cell-wall architecture [43]. Other mediators of fungal growth inhibition include pyoverdin, a bacterial siderophore that sequesters iron from the environment, and pyocyanin which disrupts the redox balance in the environment [28, 29]. Exposure of *A. fumigatus* to siderophore-deficient *P. aeruginosa* strains does not negatively impact fungal growth [48]. We used a siderophore-sufficient strain of *P. aeruginosa*, PAO1, which may in part explain the ability of these bacteria to inhibit fungal growth under the conditions we applied in this experiment. Analysis of the dataset arising from MS analysis of the bacterial secretome detected one protein associated with iron acquisition, ferric iron-binding periplasmic protein HitA.

Since gliotoxin is responsible for maintaining redox homeostasis in the fungus, an increase in gliotoxin production may be indicative of bacterial-mediated induction of reactive oxygen species, which is known to compromise fungal growth and survival [28]. Gliotoxin displays immunosuppressive effects on host cells [51–53] and thus, in the context of co-infection, the propensity of *P. aeruginosa* to promote gliotoxin production in *A. fumigatus* may have serious implications for host health.

To characterize the effect of the *P. aeruginosa* secretome on *A. fumigatus* growth and gliotoxin production, *A. fumigatus* cultures were exposed to *P. aeruginosa* CuF or *A. fumigatus* CuF for 24 h. The growth of fungal cultures when incubated with *A. fumigatus* CuF or *P. aeruginosa* CuF increased 1.36- and 2.8-fold respectively, relative to the control. Conversely, gliotoxin production was lower in fungal cultures exposed to *P. aeruginosa* CuF.

These results indicate that the response of *A. fumigatus* to *P. aeruginosa* may be regulated through direct (via bacterial cells) and indirect (via bacterial secretome) interactions with the bacteria, and that such interactions can determine hyphal formation and the secretory profile of the fungus, which may in turn have clinical significance for the host, depending on the proximity of the two pathogens to each other. Competition for nutrients such as iron, which occur when two organisms share an environment with limited resources, lead to growth inhibition of the weaker species, which, in the context of *P. aeruginosa* and *A. fumigatus*, is often the latter [28, 32, 48].

The results observed in this study contradict those observed in previous studies, in which the culture filtrates produced by *P. aeruginosa* PAO1 inhibited fungal growth [48]. However, given that the growth media used in the two studies differ in composition, this probably has implications for the biochemical profile of the secretome, and hence the effect on the fungal response in terms of growth. The positive effect of *P. aeruginosa*-mediated fungal growth has been described previously [35, 36] and the promotion of fungal growth was attributed to volatile sulphur compounds (VSCs), produced by *P. aeruginosa* on a spatially separate part of sulphur-deficient agar plates. However, bacterial VOCs can also be growth inhibitors [37]. Because VOCs can be emitted into liquid media [54], it is possible that these compounds may have had some effect on the growth of *A. fumigatus* under the culture conditions described here, but our experimental design did not allow for analysis of VOCs.

To characterize the protein profile of the *P. aeruginosa* CuF, we analysed the secretome by LFQ proteomics using high-resolution MS. Czapek-Dox liquid media can support the growth of *P. aeruginosa*, although poorly compared to other growth media due to its low nutritional content [34]. We have shown previously that the growth of *P. aeruginosa* in this medium can be promoted when conditioned in the culture filtrates produced by *A. fumigatus* in Czapek-Dox. We used MS-based proteomics to analyse the secretome of the *A. fumigatus* CuF and concluded that *A. fumigatus* creates a nutrient-rich environment which supplies *P. aeruginosa* with the nutritional components it requires to proliferate in an otherwise hostile environment [34]. Here, we used the same proteomics technique to investigate the profile of the *P. aeruginosa* secretome produced in Czapek-Dox, with a view to understanding how the bacterial culture filtrates alter the *A. fumigatus* growth and proteomic profile. We discovered a number of proteins in the dataset which provide insight as to how *P. aeruginosa* conditions this growth medium which alters fungal growth.

The glyoxylate shunt (GS) is a metabolic process whereby bacteria metabolize acetate and fatty acids as carbon sources, and which may be used as an alternative to the TCA cycle [55, 56]. This two-step pathway involves isocitrate lyase and malate synthase, and is upregulated under conditions of oxidative stress [55, 56]. Both enzymes involved in this pathway were detected in the *P. aeruginosa* CuF. The CF airways contain higher levels of fatty acids than normal airways [57] and there are indications that in the CF airways fatty acids are the main source of carbon used by *P. aeruginosa* [58].

A range of proteins involved in detoxification including catalase and thioredoxin, key components of the antioxidant system, were also detected in the culture filtrates, indicating an environmental stress response was adopted by the bacterial cells in this growth medium. Oxidative stress may be caused, in part, by low environmental pH. Bacteria can regulate the pH of their external environment to facilitate their survival [59, 60]. One way in which this may be accomplished is through the production of ammonia ions which, when combined with protons, form ammonium ions, thereby raising the pH of the environment. To achieve this, bacteria may utilize the arginine deiminase pathway, which involves the conversion of arginine to ornithine, ammonia and carbon dioxide [59, 61]. Among the enzymes involved in this process are arginine deiminase and ornithine carbamoyltransferase, both of which were detected in the dataset arising from *P. aeruginosa* CuF MS analysis. The presence of proteins involved in oxidative stress and pH regulation indicate that the bacteria modified the environment to become more conducive to growth and in doing so increased the pH of the growth media from 6.8 (pre-inoculation) to 7.2 (48 h post-inoculation). It is the higher pH and the abundance of detoxifying enzymes present in the *P. aeruginosa* CuF that may have created an environment more conducive to the growth of *A. fumigatus*, and hence greater fungal growth, compared to that created by the *A. fumigatus* CuF which had a much lower pH (4.5) and which ultimately resulted in lower fungal growth, and a significantly different proteomic profile.

To gain a better insight into the biological pathways and processes that contribute to the response of *A. fumigatus* to the *P. aeruginosa* CuF, a whole-cell proteomic approach was adopted. Modifications to histones have been extensively studied and have major implications in fungal growth and development [62, 63]. Proteomic data analysis in this study identified histone 3 as the most differentially abundant protein associated with transcriptional regulation in *A. fumigatus* cultures exposed to *P. aeruginosa* CuF (+53.81-fold). Another core component of the nucleosome, histone H2B, was detected in the group exposed to *P. aeruginosa* CuF and was increased by 2.29-fold compared to groups exposed to *A. fumigatus* CuF. In contrast, histone H2A.Z was reduced by −2.54-fold. Also reflective of changes to transcriptional and translational activity between groups was the increase in levels of proteins involved with the generation of mRNA transcripts and ribosomal activity, including ribosomal protein S28e (+18.90-fold), ribonucloprotein (+17.04-fold), 60S ribosomal protein L36 (+15.59-fold), eukaryotic translation initiation factor 4C (+4.51-fold) and RNA polymerase II subunit 3 (+2.39-fold). A decrease in the relative abundance of several ribosomal-associated proteins was also evident in the groups exposed to *P. aeruginosa* CuF. These included 40S ribosomal protein S2 (−4.31-fold) and eukaryotic translation initiation factor 3 subunit K (−3.31-fold). The increases and decreases in the relative abundance of this category of proteins highlight the changes to protein synthesis apparatus and transcriptional/translational processes that are driven by exposure to the bacterial CuF.

One of the most remarkable findings in the proteomic dataset was a significant decrease in the relative abundance of four proteins associated with the gliotoxin biosynthetic gene-cluster in *A. fumigatus* that had been exposed to *P. aeruginosa* CuF compared to *A. fumigatus* CuF. These proteins, thioredoxin reductase gliT (−53.23-fold), cytochrome P450 monooxygenase gliF (−28.47-fold), *N*-methyltransferase gliN (−21.13-fold) and glutathione *S*-transferase gliG (−12.55-fold), the gene products of gliT, gliF, gliN and gliG, respectively, were dramatically decreased in *A. fumigatus* exposed to the *P. aeruginosa* CuF. These findings correlate with those detected by RP-HPLC whereby gliotoxin production was decreased in fungal cultures grown in the presence of *P. aeruginosa* CuFs.

In contrast, analysis of the fungal proteome where *A. fumigatus* was exposed to *P. aeruginosa* CuF revealed a significant increase in the relative abundance of proteins associated with the biosynthesis of other secondary metabolites including pseurotin A (methyltransferase psoC, +49.55-fold; PKS-NRPS hybrid synthetase psoA, +24.69-fold; methyltransferase psoF; +18.35-fold, glutathione *S*-transferase psoE, +5.37-fold), verruculogen (verruculogen synthase, +44.10-fold), fumagillin (*O*-methyltransferase af390–400, +7.18-fold), and fumitremorgins (6-hydroxytryprostatin B *O*-methyltransferase, +11.45-fold; tryprostatin B synthase, +3.69-fold).

Pseurotin A is a competitive inhibitor of chitin synthase and has been reported to have cytotoxic activity, thereby highlighting its potentially cytotoxic effect on host cells [64–66]. Verruculogen and fumitremorgin b are known to affect the central nervous system *in vivo* and *in vitro*; verruculogen alters the electrophysiological properties of human nasal epithelial cells, suggesting this metabolite may participate in fungal colonization of the airways [67, 68]. Fumagillin affects the ability of neutrophils to produce superoxide anions by inhibiting the function of NADPH oxidase and prevents degranulation by interfering with the structural rearrangements required for these processes to occur [69]. An increase in the relative abundance of proteins associated with the biosynthesis of these metabolites in *A. fumigatus* coupled with a decrease in the relative abundance of gliotoxin biosynthetic proteins indicate that *P. aeruginosa* creates an environment that causes *A. fumigatus* to alter secondary metabolite production to adapt to the conditions created by the bacteria.

Contrasting results were observed in a previous study, whereby attenuation of gliotoxin biosynthesis by deletion of the gliotoxin bis-thiomethyltransferase gene, GtmA, corresponded to a decrease in the levels of pseurotinA, fumagillin, tryprostatin B and fumitremorgin C [70]. The findings of both studies highlight the complexities involved in the regulation of secondary metabolite biosynthesis, and demonstrate that their induction at a molecular level may be controlled by multiple environmental stimuli.

An increase in the relative abundance of proteins associated with an oxidative stress response and detoxification (formate dehydrogenase, +18.64-fold; thioredoxin reductase, +43.91-fold; AhpC/TSA family protein, +6.51-fold; catalase-peroxidase, +3.64-fold) was

detected in the *A. fumigatus* proteome where the fungus was exposed to the *P. aeruginosa* CuF [71–73]. This suggests that the contents of *P. aeruginosa* CuF induce oxidative stress in *A. fumigatus*.

The proteomic data also revealed a decrease in the relative abundance of several proteins associated with the mitochondria in *A. fumigatus* exposed to *P. aeruginosa* CuF compared with that exposed to *A. fumigatus* CuF. Alterations to the mitochondria are indicative of an increase in energy production and oxidative stress. The proteins detected here were involved with complex III of the respiratory transport-chain and included succinate dehydrogenase cytochrome b560 subunit (−8.45-fold), ubiquinol-cytochrome *c* reductase complex 17 kd protein (−5.85-fold), cytochrome C (−1.94-fold) and cytochrome *b-c*1 complex subunit 7 (−1.83-fold). Oxidative stress induces the release of cytochrome *c* from the mitochondria and is a signature of mitochondrial dysfunction [74]. The increased levels of proteins associated with cytochrome complexes in the group exposed to *A. fumigatus* CuF correlate with the increased levels of proteins associated with gliotoxin biosynthesis in these fungal cultures. Gliotoxin is a driver of oxidative stress in the microenvironment and a known contributor to mitochondrial stress, which may explain why indicators of mitochondrial dysfunction are observed in the group exposed to *A. fumigatus* CuF to a greater extent than those exposed to *P. aeruginosa* CuF [75–78]. These data indicate that the stress response induced by *P. aeruginosa* CuF differs to that which is induced by *A. fumigatus* CuF and, given that certain virulence factors are often dependent upon the type of stress response endured by the pathogen [79], suggests potential implications during instances of co-infection.

A. fumigatus secretes a range of degradative enzymes that contribute to the ubiquity of the fungus in nature by supporting fungal growth on plant matter [4, 5]. Many of these biological determinants also play a role in establishing disease in humans and are associated with virulence and pathogenesis. Several proteases involved in conidial development, and also thought to play a role in ABPA were detected in the data set presented here, including alkaline protease 2 (+2.42-fold), major allergen Asp f 2 (+2.26-fold) and vacuolar protease A (+2.09-fold) [80, 81]. The increase in relative abundance of these enzymes, due to exposure by *P. aeruginosa* CuF, suggests that the presence of bacterial-derived molecules in the environment potentially promote the expression of the genes encoding such proteins.

CONCLUSION

In the CF airways, *A. fumigatus* rarely becomes invasive as germinating conidia are rapidly targeted by cells of the immune system [82, 83]. However, if hyphae are produced, antigens, proteases and other factors that induce an inflammatory response can be released [83]. Because *P. aeruginosa* is prevalent in the CF airways, it is important to understand the role of bacteria in influencing fungal growth and development. The data presented here indicate that the secreted products of *P. aeruginosa* can influence the proteomic response of *A. fumigatus* and, consequently, the effect of the fungus on the host, by way of modulating secondary metabolite production. The role of *A. fumigatus* proteases in exacerbating pulmonary disorders such as ABPA have been established, but with the exception of gliotoxin, less is known about the effects of other secondary metabolites (e.g. pseurotin A) on the immune system. Given the prevalence of *A. fumigatus* as an infectious agent and its propensity to co-infect the airways with other pathogens, it may be of interest to investigate whether other bacteria induce similar responses in terms of mycotoxin production.

Funding information
Anatte Margalit is the recipient of an Irish Research Council Doctoral scholarship. David Sheehan was funded by a Wellcome Trust Biomedical Vacation 26 Scholarship (Scholarship number: WELLCOME 213358/Z/18Z_SHEEHAN). The Q-exactive mass spectrometer was funded under the SFI Research Infrastructure Call 2012; Grant Number: 12/RI/2346 (3).

Conflicts of interest
The authors declare that there are no conflicts of interest.

References

1. Vivek-Ananth RP, Mohanraj K, Vandanashree M, Jhingran A, Craig JP, *et al*. Comparative systems analysis of the secretome of the opportunistic pathogen *Aspergillus fumigatus* and other *Aspergillus* species. *Sci Rep* 2018;8:6617.
2. Wartenberg D, Lapp K, Jacobsen ID, Dahse H-M, Kniemeyer O, *et al*. Secretome analysis of *Aspergillus fumigatus* reveals Asp-hemolysin as a major secreted protein. *Int J Med Microbiol* 2011;301:602–611.
3. Behnsen J, Lessing F, Schindler S, Wartenberg D, Jacobsen ID, *et al*. Secreted *Aspergillus fumigatus* protease Alp1 degrades human complement proteins C3, C4, and C5. *Infect Immun* 2010;78:3585–3594.
4. Wang D, Zhang L, Zou H, Wang L. Secretome profiling reveals temperature-dependent growth of *Aspergillus fumigatus*. *Sci China Life Sci* 2018;61:578–592.
5. Tekaia F, Latgé J-P. *Aspergillus fumigatus*: saprophyte or pathogen? *Curr Opin Microbiol* 2005;8:385–392.
6. Paulussen C, Hallsworth JE, Álvarez-Pérez S, Nierman WC, Hamill PG, *et al*. Ecology of aspergillosis: insights into the pathogenic potency of *Aspergillus fumigatus* and some other *Aspergillus* species. *Microb Biotechnol* 2017;10:296–322.
7. Bignell E, Cairns TC, Throckmorton K, Nierman WC, Keller NP. Secondary metabolite arsenal of an opportunistic pathogenic fungus. *Phil Trans R Soc B* 2016;371:20160023.
8. Inglis DO, Binkley J, Skrzypek MS, Arnaud MB, Cerqueira GC, *et al*. Comprehensive annotation of secondary metabolite biosynthetic genes and gene clusters of *Aspergillus nidulans*, *A. fumigatus*, *A. niger* and *A. oryzae*. *BMC Microbiol* 2013;13:91.
9. Raffa N, Keller NP, Sheppard DC. A call to arms: Mustering secondary metabolites for success and survival of an opportunistic pathogen. *PLOS Pathog* 2019;15:e1007606.
10. Amin S, Thywissen A, Heinekamp T, Saluz HP, Brakhage AA. Melanin dependent survival of *Apergillus fumigatus* conidia in lung epithelial cells. *Int J Med Microbiol* 2014;304:626–636.

11. Fallon JP, Reeves EP, Kavanagh K. Inhibition of neutrophil function following exposure to the *Aspergillus fumigatus* toxin fumagillin. *J Med Microbiol* 2010;59:625–633.
12. Schlam D, Canton J, Carreño M, Kopinski H, Freeman SA, *et al*. Gliotoxin suppresses macrophage immune function by subverting phosphatidylinositol 3,4,5-trisphosphate homeostasis. *mBio* 2016;7:1–15.
13. Coburn B, Wang PW, Diaz Caballero J, Clark ST, Brahma V, *et al*. Lung microbiota across age and disease stage in cystic fibrosis. *Sci Rep* 2015;5:10241.
14. Breuer O, Schultz A, Garratt LW, Turkovic L, Rosenow T, *et al*. *Aspergillus* infections and progression of structural lung disease in children with cystic fibrosis. *Am J Respir Crit Care Med* 2020;201:688–696.
15. Reece E, McClean S, Greally P, Renwick J. The prevalence of *Aspergillus fumigatus* in early cystic fibrosis disease is underestimated by culture-based diagnostic methods. *J Microbiol Methods* 2019;164:105683.
16. Stevens DA, Moss RB, Kurup VP, Knutsen AP, Greenberger P, *et al*. Allergic bronchopulmonary aspergillosis in cystic fibrosis--state of the art: Cystic Fibrosis Foundation Consensus Conference. *Clin Infect Dis* 2003;37 Suppl 3:S225-64.
17. Maturu VN, Agarwal R. Prevalence of *Aspergillus* sensitization and allergic bronchopulmonary aspergillosis in cystic fibrosis: systematic review and meta-analysis. *Clin Exp Allergy* 2015;45:1765–1778.
18. Denning DW, Pleuvry A, Cole DC. Global burden of allergic bronchopulmonary aspergillosis with asthma and its complication chronic pulmonary aspergillosis in adults. *Med Mycol* 2013;51:361–370.
19. Armstead J, Morris J, Denning DW. Multi-country estimate of different manifestations of aspergillosis in cystic fibrosis. *PLOS ONE* 2014;9:e98502.
20. Reece E, Segurado R, Jackson A, McClean S, Renwick J, *et al*. Co-colonisation with *Aspergillus fumigatus* and *Pseudomonas aeruginosa* is associated with poorer health in cystic fibrosis patients: an Irish registry analysis. *BMC Pulm Med* 2017;17:1–8.
21. Zhao J, Cheng W, He X, Liu Y. The co-colonization prevalence of *Pseudomonas aeruginosa* and *Aspergillus fumigatus* in cystic fibrosis: A systematic review and meta-analysis. *Microb Pathog* 2018;125:122–128.
22. Fothergill JL, Walshaw MJ, Winstanley C. Transmissible strains of *Pseudomonas aeruginosa* in cystic fibrosis lung infections. *Eur Respir J* 2012;40:227–238.
23. Hector A, Kirn T, Ralhan A, Graepler-Mainka U, Berenbrinker S, *et al*. Microbial colonization and lung function in adolescents with cystic fibrosis. *J Cyst Fibros* 2016;15:340–349.
24. Reece E, Segurado R, Jackson A, McClean S, Renwick J, *et al*. Co-colonisation with *Aspergillus fumigatus* and *Pseudomonas aeruginosa* is associated with poorer health in cystic fibrosis patients: an Irish registry analysis. *BMC Pulm Med* 2017;17:70.
25. Zhao J, Cheng W, He X, Liu Y. The co-colonization prevalence of *Pseudomonas aeruginosa* and *Aspergillus fumigatus* in cystic fibrosis: A systematic review and meta-analysis. *Microb Pathog* 2018;125:122–128.
26. Paugam A, Baixench M-T, Demazes-Dufeu N, Burgel P-R, Sauter E, *et al*. Characteristics and consequences of airway colonization by filamentous fungi in 201 adult patients with cystic fibrosis in France. *Med Mycol* 2010;48 Suppl 1:S32-6.
27. Yonezawa M, Sugiyama H, Kizawa K, Hori R, Mitsuyama J, *et al*. A new model of pulmonary superinfection with *Aspergillus fumigatus* and *Pseudomonas aeruginosa* in mice. *J Infect Chemother* 2000;6:155–161.
28. Briard B, Bomme P, Lechner BE, Mislin GLA, Lair V, *et al*. *Pseudomonas aeruginosa* manipulates redox and iron homeostasis of its microbiota partner *Aspergillus fumigatus* via phenazines. *Sci Rep* 2015;5:8220.
29. Sass G, Nazik H, Penner J, Shah H, Ansari SR, *et al*. Studies of *Pseudomonas aeruginosa* mutants indicate pyoverdine as the central factor in inhibition of *Aspergillus fumigatus* biofilm. *J Bacteriol* 2018;200:1–24.
30. Shirazi F, Ferreira JAG, Stevens DA, Clemons KV, Kontoyiannis DP. Biofilm filtrates of *Pseudomonas aeruginosa* strains isolated from cystic fibrosis patients inhibit preformed *Aspergillus fumigatus* biofilms via apoptosis. *PLoS One* 2016;11:e0150155.
31. Ferreira JAG, Penner JC, Moss RB, Haagensen JAJ, Clemons KV, *et al*. Inhibition of *Aspergillus fumigatus* and its biofilm by *Pseudomonas aeruginosa* is dependent on the source, phenotype and growth conditions of the bacterium. *PLOS ONE* 2015;10:e0134692.
32. Mowat E, Rajendran R, Williams C, McCulloch E, Jones B, *et al*. *Pseudomonas aeruginosa* and their small diffusible extracellular molecules inhibit *Aspergillus fumigatus* biofilm formation. *FEMS Microbiology Letters* 2010;313:96–102.
33. Reece E, Doyle S, Greally P, Renwick J, McClean S. *Aspergillus fumigatus* inhibits *Pseudomonas aeruginosa* in co-culture: implications of a mutually antagonistic relationship on virulence and inflammation in the CF airway. *Front Microbiol* 2018;9:1–14.
34. Margalit A, Carolan JC, Sheehan D, Kavanagh K. The *Aspergillus fumigatus* secretome alters the proteome of *Pseudomonas aeruginosa* to stimulate bacterial growth: implications for co-infection. *Molecular & Cellular Proteomics* 2020;19:1346–1359.
35. Briard B, Heddergott C, Latgé J-P, Taylor JW, Dunlap JC, *et al*. Volatile compounds emitted by *Pseudomonas aeruginosa* stimulate growth of the fungal pathogen *Aspergillus fumigatus*. *mBio* 2016;7:1–5.
36. Scott J, Sueiro-Olivares M, Ahmed W, Heddergott C, Zhao C, *et al*. *Pseudomonas aeruginosa*-derived volatile sulfur compounds promote distal *Aspergillus fumigatus* growth and a synergistic pathogen-pathogen interaction that increases pathogenicity in co-infection. *Front Microbiol* 2019;10:2311.
37. Nazik H, Sass G, Déziel E, Stevens DA. *Aspergillus* is inhibited by *Pseudomonas aeruginosa* volatiles. *JoF* 2020;6:118.
38. Smith K, Rajendran R, Kerr S, Lappin DF, Mackay WG, *et al*. *Aspergillus fumigatus* enhances elastase production in *Pseudomonas aeruginosa* co-cultures. *Med Mycol* 2015;53:645–655.
39. Sass G, Ansari SR, Dietl A-M, Déziel E, Haas H, *et al*. Intermicrobial interaction: *Aspergillus fumigatus* siderophores protect against competition by *Pseudomonas aeruginosa*. *PLoS One* 2019;14:e0216085.
40. Hubner NC, Bird AW, Cox J, Splettstoesser B, Bandilla P, *et al*. Quantitative proteomics combined with BAC TransgeneOmics reveals in vivo protein interactions. *J Cell Biol* 2010;189:739–754.
41. Côté RG, Griss J, Dianes JA, Wang R, Wright JC, *et al*. The PRoteomics IDEntification (PRIDE) converter 2 framework: an improved suite of tools to facilitate data submission to the PRIDE Database and the ProteomeXchange Consortium. *Molecular & Cellular Proteomics* 2012;11:1682–1689.
42. Murphy S, Zweyer M, Mundegar RR, Swandulla D, Ohlendieck K. Proteomic identification of elevated saliva kallikrein levels in the *mdx-4cv* mouse model of Duchenne muscular dystrophy. *Biochem Biophys Rep* 2019;18:100541.
43. Briard B, Rasoldier V, Bomme P, ElAouad N, Guerreiro C, *et al*. Dirhamnolipids secreted from *Pseudomonas aeruginosa* modify anjpegungal susceptibility of *Aspergillus fumigatus* by inhibiting β1,3 glucan synthase activity. *ISME J* 2017;11:1578–1591.
44. Briard B, Mislin GLA, Latgé J-P, Beauvais A. Interactions between *Aspergillus fumigatus* and pulmonary bacteria: current state of the field, new data, and future perspective. *J Fungi (Basel)* 2019;5:48.
45. Cramer RA, Gamcsik MP, Brooking RM, Najvar LK, Kirkpatrick WR, *et al*. Disruption of a nonribosomal peptide synthetase in *Aspergillus fumigatus* eliminates gliotoxin production . *Eukaryot Cell* 2006;5:972–980.
46. Dolan SK, Owens RA, O'Keeffe G, Hammel S, Fitzpatrick DA, *et al*. Regulation of nonribosomal peptide synthesis: bis-thiomethylation attenuates gliotoxin biosynthesis in *Aspergillus fumigatus*. *Chem Biol* 2014;21:999–1012.
47. Line L, Alhede M, Kolpen M, Kühl M, Ciofu O, *et al*. Physiological levels of nitrate support anoxic growth by denitrification of

Pseudomonas aeruginosa at growth rates reported in cystic fibrosis lungs and sputum. *Front Microbiol* 2014;5:554.

48. Wurster S, Sass G, Albert ND, Nazik H, Déziel E, *et al*. Live imaging and quantitative analysis of *Aspergillus fumigatus* growth and morphology during inter-microbial interaction with *Pseudomonas aeruginosa Virulence* 2020;11:1329–1336.
49. Margalit A, Carolan JC, Kavanagh K. Bacterial Interactions with *Aspergillus fumigatus* in the Immunocompromised Lung. *Microorganisms* 2021;9:435.
50. Abalos A, Pinazo A, Infante MR, Casals M, García F, *et al*. Physicochemical and antimicrobial properties of new rhamnolipids produced by *Pseudomonas a eruginosa* AT10 from soybean oil refinery wastes. *Langmuir* 2001;17:1367–1371.
51. Stanzani M, Orciuolo E, Lewis R, Kontoyiannis DP, Martins SLR, *et al*. *Aspergillus fumigatus* suppresses the human cellular immune response via gliotoxin-mediated apoptosis of monocytes. *Blood* 2005;105:2258–2265.
52. Schlam D, Canton J, Carreño M, Kopinski H, Freeman SA, *et al*. Gliotoxin suppresses macrophage immune function by subverting phosphatidylinositol 3,4,5-trisphosphate homeostasis. *mBio* 2016;7:e02242.
53. Orciuolo E, Stanzani M, Canestraro M, Galimberti S, Carulli G, *et al*. Effects of *Aspergillus fumigatus* gliotoxin and methylprednisolone on human neutrophils: implications for the pathogenesis of invasive aspergillosis. *J Leukoc Biol* 2007;82:839–848.
54. Reese KL, Rasley A, Avila JR, Jones AD, Frank M. Metabolic Profiling of Volatile Organic Compounds (VOCs) emitted by the pathogens *Francisella tularensis* and *Bacillus anthracis* in liquid culture. *Sci Rep* 2020;10:9333.
55. da Cruz Nizer WS, Inkovskiy V, Versey Z, Strempel N, Cassol E, *et al*. Oxidative stress response in *Pseudomonas aeruginosa*. *Pathogens* 2021;10:1187.
56. Ahn S, Jung J, Jang I-A, Madsen EL, Park W. Role of glyoxylate shunt in oxidative stress response. *J Biol Chem* 2016;291:11928–11938.
57. Meyer KC, Sharma A, Brown R, Weatherly M, Moya FR, *et al*. Function and composition of pulmonary surfactant and surfactant-derived fatty acid profiles are altered in young adults with cystic fibrosis. *Chest* 2000;118:164–174.
58. Son MS, Matthews WJ Jr, Kang Y, Nguyen DT, Hoang TT. *In vivo* evidence of *Pseudomonas aeruginosa* nutrient acquisition and pathogenesis in the lungs of cystic fibrosis patients. *Infect Immun* 2007;75:5313–5324.
59. Lund P, Tramonti A, De Biase D. Coping with low pH: molecular strategies in neutralophilic bacteria. *FEMS Microbiol Rev* 2014;38:1091–1125.
60. Ratzke C, Gore J. Modifying and reacting to the environmental pH can drive bacterial interactions. *PLoS Biol* 2018;16:e2004248.
61. Cunin R, Glansdorff N, Piérard A, Stalon V. Biosynthesis and metabolism of arginine in bacteria. *Microbiol Rev* 1986;50:314–352.
62. Brosch G, Loidl P, Graessle S. Histone modifications and chromatin dynamics: a focus on filamentous fungi. *FEMS Microbiol Rev* 2008;32:409–439.
63. Palmer JM, Perrin RM, Dagenais TRT, Keller NP. H3K9 methylation regulates growth and development in *Aspergillus fumigatus*. *Eukaryot Cell* 2008;7:2052–2060.
64. Bladt TT, Frisvad JC, Knudsen PB, Larsen TO. Anticancer and antifungal compounds from *Aspergillus*, *Penicillium* and other filamentous fungi. *Molecules* 2013;18:11338–11376.
65. Martínez-Luis S, Cherigo L, Arnold E, Spadafora C, Gerwick WH, *et al*. Antiparasitic and anticancer constituents of the endophytic fungus *Aspergillus* sp. strain F1544. *Nat Prod Commun* 2012;7:1934578X1200700.
66. Wenke J, Anke H, Sterner O. Pseurotin A and 8- O -Demethylpseurotin A from *Aspergillus fumigatus* and their inhibitory activities on chitin synthase. *Biosci Biotechnol Biochem* 2014;57:961–964.
67. Khoufache K, Puel O, Loiseau N, Delaforge M, Rivollet D, *et al*. Verruculogen associated with *Aspergillus fumigatus* hyphae and conidia modifies the electrophysiological properties of human nasal epithelial cells. *BMC Microbiol* 2007;7:5.
68. Tepšič K, Gunde-Cimerman N, Frisvad JC. Growth and mycotoxin production by *Aspergillus fumigatus* strains isolated from a saltern. *FEMS Microbiology Letters* 2006;157:9–12.
69. Fallon JP, Reeves EP, Kavanagh K. Inhibition of neutrophil function following exposure to the *Aspergillus fumigatus* toxin fumagillin. *J Med Microbiol* 2010;59:625–633.
70. Doyle S, Jones GW, Dolan SK. Dysregulated gliotoxin biosynthesis attenuates the production of unrelated biosynthetic gene cluster-encoded metabolites in *Aspergillus fumigatus*. *Fungal Biol* 2018;122:214–221.
71. Sugui JA, Kim HS, Zarember KA, Chang YC, Gallin JI, *et al*. Genes differentially expressed in conidia and hyphae of *Aspergillus fumigatus* upon exposure to human neutrophils. *PLOS ONE* 2008;3:e2655.
72. Marshall AC, Kidd SE, Lamont-Friedrich SJ, Arentz G, Hoffmann P, *et al*. Structure, mechanism, and inhibition of *Aspergillus fumigatus* thioredoxin reductase. *Antimicrob Agents Chemother* 2019;63:e02281-18.
73. Paris S, Wysong D, Debeaupuis J-P, Shibuya K, Philippe B, *et al*. Catalases of *Aspergillus fumigatus*. *Infect Immun* 2003;71:3551–3562.
74. Li L, Hu X, Xia Y, Xiao G, Zheng P, *et al*. Linkage of oxidative stress and mitochondrial dysfunctions to spontaneous culture degeneration in *Aspergillus nidulans*. *Mol Cell Proteomics* 2014;13:449–461.
75. Gayathri L, Akbarsha MA, Ruckmani K. In vitro study on aspects of molecular mechanisms underlying invasive aspergillosis caused by gliotoxin and fumagillin, alone and in combination. *Sci Rep* 2020;10:14473.
76. Islam MT, Mishra SK, Tripathi S, de Alencar MVOB, E Sousa JM de C, *et al*. Mycotoxin-assisted mitochondrial dysfunction and cytotoxicity: Unexploited tools against proliferative disorders. *IUBMB Life* 2018;70:1084–1092.
77. Gallagher L, Owens RA, Dolan SK, O'Keeffe G, Schrettl M, *et al*. The *Aspergillus fumigatus* protein GliK protects against oxidative stress and is essential for gliotoxin biosynthesis. *Eukaryot Cell* 2012;11:1226–1238.
78. Schrettl M, Carberry S, Kavanagh K, Haas H, Jones GW, *et al*. Self-protection against gliotoxin--a component of the gliotoxin biosynthetic cluster, GliT, completely protects *Aspergillus fumigatus* against exogenous gliotoxin. *PLoS Pathog* 2010;6:e1000952.
79. Fang FC, Frawley ER, Tapscott T, Vázquez-Torres A. Bacterial stress responses during host infection. *Cell Host Microbe* 2016;20:133–143.
80. Abad A, Fernández-Molina JV, Bikandi J, Ramírez A, Margareto J, *et al*. What makes *Aspergillus fumigatus* a successful pathogen? Genes and molecules involved in invasive aspergillosis. *Rev Iberoam Micol* 2010;27:155–182.
81. Reichard U, Cole GT, Hill TW, Rüchel R, Monod M. Molecular characterization and influence on fungal development of ALP2, a novel serine proteinase from *Aspergillus fumigatus*. *Int J Med Microbiol* 2000;290:549–558.
82. Burgel P-R, Paugam A, Hubert D, Martin C. *Aspergillus fumigatus* in the cystic fibrosis lung: pros and cons of azole therapy. *Infect Drug Resist* 2016;9:229–238.
83. Dagenais TRT, Keller NP. Pathogenesis of *Aspergillus fumigatus* in invasive *Aspergillosis*. *Clin Microbiol Rev* 2009;22:447–465.

Edited by: H. Sychrova and R. Hall